Pd-Catalyzed Homocoupling Reaction of Arylboronic Acid: Insights from Density Functional Theory†

H. Lakmini,§ I. Ciofini,‡ A. Jutand,§ C. Amatore,§ and C. Adamo*,‡

Laboratoire d'Electrochimie et Chimie Analytique, Ecole Nationale Supérieure de Chimie, UMR CNRS 7575, 11 Rue Pierre et Marie Curie, F-75231 Paris Cedex 5, France, and Département de Chimie, Ecole Normale Supérieure, UMR CNRS-ENS-UPMC 8640, 24 Rue Lhomond, F-75231 Paris Cedex 5, France

Received: March 5, 2008; Revised Manuscript Received: April 17, 2008

The key step in the mechanism of the Palladium-catalyzed homocoupling of arylboronic acids $ArB(OH)_2$ (Ar = 4-Z-C_6H_4 with Z = MeO, H, CN) in the presence of dioxygen, leading to symmetrical biaryls, has been elucidated by using density functional theory. In particular, by starting from the peroxo complex O_2PdL_2 (L = PPh_3), generated in the reaction of dioxygen with the Pd(0) catalyst, the fundamental role played by an intermediate formed by coordination of one oxygen atom of the peroxo complex to the oxophilic boron atom of the arylboronic acid has been pointed out. This adduct reacts with a second molecule of arylboronic acid to generate a *cis*-Ar-Pd(OOB$(OH)_2$)L_2 complex that can form the stable intermediate *trans*-Ar-Pd$(OH)L_2$ (experimentally characterized) through a sequence of hydrolysis and isomerization reactions. All theoretical insights are in agreement and do substantiate the experimentally postulated mechanism. Furthermore, direct comparison of experimental and computed spectroscopic parameters (here, ^{31}P chemical shifts) allows us to confirm the formation of the intermediate.

Introduction

Palladium-catalyzed coupling reactions are nowadays one of the most widely used methods to form sp^2-sp^2 carbon−carbon bonds. In particular, cross-coupling reaction of arylboronic acids $ArB(OH)_2$ or esters $ArB(OR)_2$ with aryl derivatives, Ar′X, allows us to obtain unsymmetrical biaryls ArAr′[1] in the Miyaura−Suzuki reactions[2] (Scheme 1).

Beside the formation of the major cross-coupling product Ar′Ar, a minor byproduct ArAr may be observed that is formed in a palladium-catalyzed homocoupling of $ArB(OZ)_2$ (Z = H or R).[2,3] More recently, the palladium-catalyzed homocoupling of arylboronic acids or esters was developed as a main reaction when performed in the presence of a chemical oxidant[4] or pure dioxygen or air[5,6] (Scheme 2). The homocoupling of arylboronic acids was first reported by Moreno-Mañas et al. in 1996 by using Pd(0) or Pd(II) catalysts associated with monodentate phosphines.[5] The homocoupling was later extended to arylboronic esters by Yoshida et al. in 2003 by using $Pd(OAc)_2$ as catalyst and dppp (1,3-bis-(diphenylphosphino)propane) as ligand.[7]

Very little is known about the reaction mechanism of this oxidative homocoupling. A first mechanism was proposed, involving the oxidative addition of $ArB(OH)_2$ to Pd(0) complexes with the generation of $ArPd^{II}-[B(OH)_2]L_2$ (L = PPh_3).[5] Sheldon and Kochi have suggested the formation of the intermediate complex Ar_2PdL_2 (L = PPh_3) by a double transmetallation of $ArB(OH)_2$ on (HO)Pd(OOH)L_2, generated by reaction of water with the peroxo complex O_2PdL_2.[8] Yoshida et al. proposed a reaction of arylboronic esters $ArB(OR)_2$ with O_2Pd(dppp), which would give ArPd−[OOB$(OR)_2$](dppp).[7] A subsequent transmetallation on the latter complex by $ArB(OR)_2$ would give Ar_2Pd(dppp) and the homocoupling product ArAr by a reductive elimination.

SCHEME 1

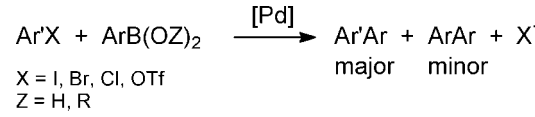

SCHEME 2

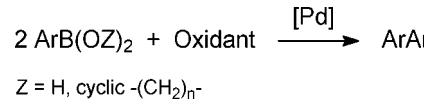

Very recently, we mechanistically and kinetically established that a peroxo complex of palladium, O_2PdL_2 (L = PPh_3),[9] plays a key role in the catalytic homocoupling of arylboronic acids, and we proposed a catalytic cycle schematically depicted in Figure 1, on the basis of experimental studies, confirmed by preliminary ab initio results.[10]

Indeed, only for a few intermediates does experimental evidence (i.e. NMR spectra and kinetics) exist.

The aim of the present work is to further confirm the proposed cycle from a theoretical point of view. In particular, we focused on the first part of the catalytic cycle and tried to define the elementary steps leading to the formation of complex **5** because once this system is formed, a transmetallation by the arylboronic acid would give *trans*-$ArPdArL_2$ complexes, and the biaryl could be simply released by reductive elimination.

To this end, density functional theory (DFT) was applied to determine the structural, energetic, and spectroscopic signatures, when available, of the catalytic cycle. This method,[11] in particular in conjunction with hybrid exchange-correlation functionals, has become one of the major theoretical tools of quantum chemistry, notably thanks to its reliability, its low computational cost, and its range of applications. For these

† Part of the "Sason S. Shaik Festschrift".

* Corresponding author. E-mail: carlo-adamo@enscp.fr.
§ UMR CNRS-ENS-UPMC 8640.
‡ UMR CNRS 7575.

10.1021/jp801948u CCC: $40.75
Published on Web 07/02/2008

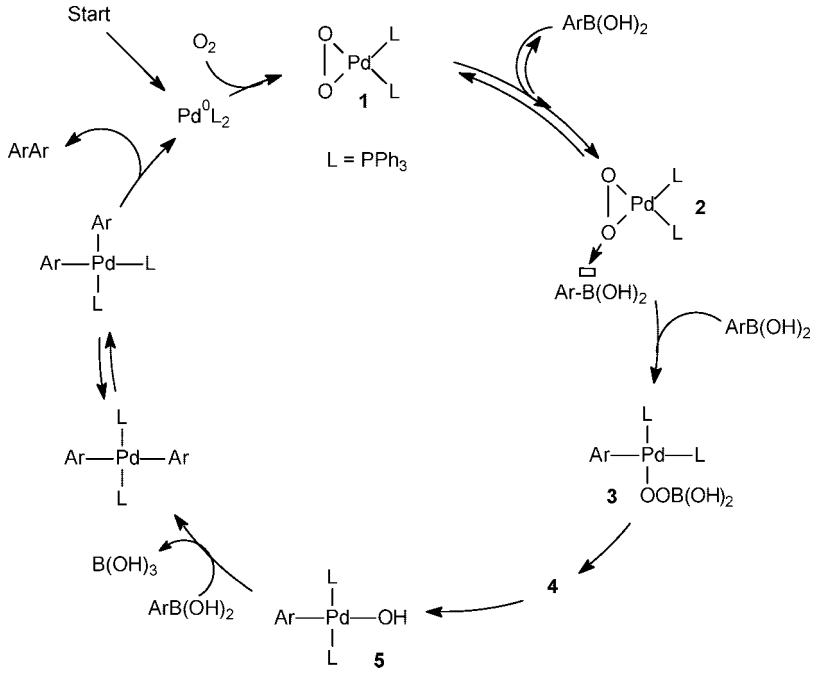

Figure 1. Proposed mechanism for the homocoupling of arylboronic acid catalysed by the peroxo complex.[10]

reasons, such an approach has been successfully applied to the study of a large number of catalytic reactions for more than a decade (see for instance ref 12). In particular, seminal computational works performed at DFT level by Shaik and collaborators allowed to clearly elucidate the role of anionic zero-valent palladium catalysts in Heck and cross-coupling reactions (see for instance ref 13), thus already pointing out the excellent performance of this method for the prediction and interpretation of Pd-based catalytic reactions.

In this context, we aimed at pointing out the key role played by the intermediate **2** formed by coordination of one oxygen atom of the peroxo complex to the oxophilic boron atom of the arylboronic acid. Furthermore, the reaction mechanism leading to the reaction of this adducts with a second molecule of arylboronic acid to generate a four-center transition state has been characterized. In such a way, a consistent explanation of the formation of the stable intermediate *trans*-Ar-Pd(OH))L_2 (experimentally characterized) through a sequence of successive hydrolysis and isomerization reactions is theoretically given.

Finally, the comparison of computed and experimental NMR signatures of the formation of complex **2** allows to further validate the proposed mechanism.

Computational Details

All calculations were carried out by using the Gaussian code.[14] A hybrid Hartree−Fock/density functional model (HF/DFT), hereafter referred to as PBE0, was used throughout.[15] In this functional, derived from the PBE,[16] the ratio of HF/DFT exchange is fixed a priori to 1/4.[17] A double ζ quality LANL2 basis[18] and corresponding relativistic pseudo-potential (including mass velocity and Darwin terms)[19] was used for all calculations. Such level of theory was proven to provide reliable results for thermochemical and spectroscopic properties as well as reactivity.[20] No symmetry constraints were imposed during structural optimizations, and the nature of the optimized structures, energy minima, was defined by subsequent frequency calculations. All reaction energies are referred to those of separated reactants,[21] and enthalpies variations (ΔH) are computed in standard conditions (298.15 K and 1 Atm). NMR calculations were performed by using the GIAO approach[22] and an ad hoc basis set, see below.

Solvent effects were simulated by using an implicit solvation model based on the polarizable continuum model (PCM) of Tomasi and co-workers.[23] More specifically, the conductor-like PCM model (CPCM) in conjunction with the united atom topological model (using UA0 radii), as implemented in Gaussian03,[24,25] was applied. Two different solvents ($CHCl_3$, $\varepsilon = 4.90$ and water, $\varepsilon = 78.39$) were considered. Explicit solute−solvent interaction, that is, explicit consideration of solvent molecules, was always neglected.

Results and Discussion

Figure 2 shows sketches of the stable intermediates (**1**, **2**, **3**, **4a**, **4b**, and **5**) and the transition state (**TS1**) computed in the gas phase for Ar = Ph. For the sake of clarity, in the following, each step of the overall mechanism will be separately discussed. Indeed, it is worth noting that up to complex **5**, the catalytic cycle is computed to be, on the whole, strongly exothermic (−64.3 kJ/mol).

Step 1: Formation of Complex 2. As the first step of the mechanism, the arylboronic acid (**A** = $ArB(OH)_2$, Ar = 4-Z-C_6H_4) coordinates to the palladium complex (**1**) via a classical Lewis acid−base interaction between an oxygen atom of the peroxo complex (**1**) and the boron atom of **A**. This interaction leads to a stable intermediate (**2,** Figure 3), the reaction being exothermic ($\Delta H = -31.8$ for Ar = Ph). To test the dependence of the reaction upon the Lewis acidity of **A**, Z was varied from an electron-donating group (MeO) to H to an electron-withdrawing substituent (CN).

From a structural point of view, the main effect of the interaction between **A** and **1** is that the coordination sphere of the boron atom changes from trivalent-planar in the isolated **A** to practically tetrahedral in complex **2**. In fact, the boron oxygen bond lengths computed for **2** (1.452−1.455 Å, Table 1) are consistent with values reported in the literature for boron−ligand distances in boronate complexes (1.556 Å).[26]

The formation of **2** also leads to a significant elongation (up to ∼0.1 Å) of the Pd−O bond for the oxygen atom interacting

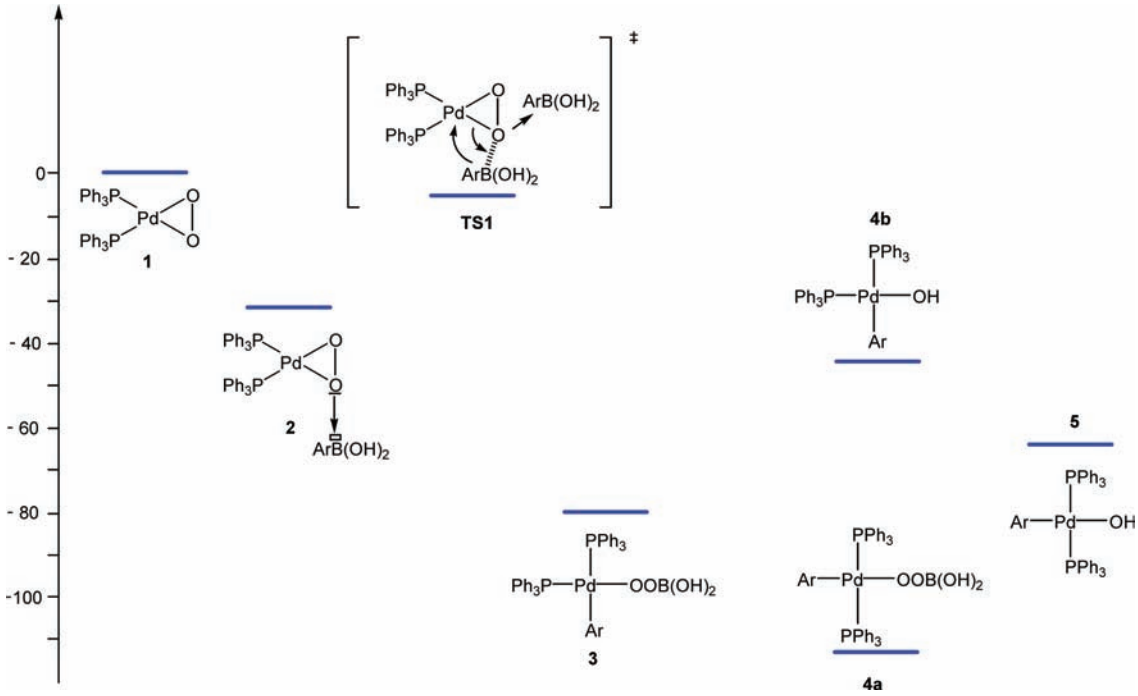

Figure 2. Relative enthalpies (ΔH, in kJ/mol) and representations of the stable intermediates and transition state, computed in the gas phase, for Ar=Ph.

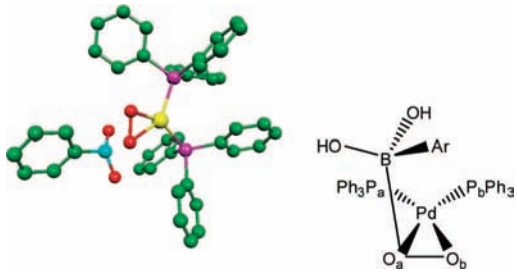

Figure 3. Computed optimized structure of **2** (left, Ar = Ph; hydrogen atoms omitted for clarity) along with its schematic representation and labeling (right).

with the boron (i.e., O_a, Figure 3). This lengthening is proportional to the electron-withdrawing strength of the Z group on the arylboronic acid. In particular, it increases for Z going from MeO to H to CN. Analogously, the oxygen−oxygen bond length is elongated by ∼0.1 Å.

On the contrary, the phosphine ligands are not strongly affected by the formation of the dative complex **2**, the variation of the Pd−P bonds being smaller than 0.04 Å and that of the PPdP angles always lower than 2°. These results are in agreement with NMR experimental insights, see below.

From a thermodynamic point of view, we assume that the formation of complex **2** in the gas phase is practically barrierless; thus, no attempts to locate transition states have been performed. Furthermore, because of the well-known high oxophilicity of boron centers, the exothermic formation of **2** is not surprising. We can also expect that the reaction energy will be tuned if the arylboronic acid is functionalized with an electron withdrawing group. To test this dependence, the formation energy of **2** as a function of the Z substituent on the arylboronic acid is reported in Table 2. It appears that, although this reaction is exothermic for all Z in the gas phase, the highest formation energy is computed for Z = CN. The stability of **2** practically doubles when going from an electron-donating substituent on the arylboronic acid (Z = MeO, ΔH = −26.8 kJ/mol) to an electron-withdrawing group such as Z = CN (ΔH = −49.4 kJ/mol). All these data are in agreement with kinetics measurements.[10]

In particular, because there is experimental evidence, from kinetics measurements, that the formation of complex **2** is thermodynamically governed, one can compare the overall enthalpies of formation (ΔH, Table 2) with the reaction rate constant experimentally extracted from kinetics measurements. One finds that the computed data (ΔH) are fully in line with the experimental trends.[10]

From an experimental point of view, the formation of complex **2** was further supported by the analysis of ^{11}B and ^{31}P NMR spectra obtained when a sub-stoichiometry quantity of arylboronic acid is added to a solution of the peroxo complex **1**. Under these conditions, in the ^{31}P NMR spectrum, beside the singlet signal due to the presence of **1**, two doublets appear at lower frequency (Table 3). These two doublets indicate the presence of a new complex possessing two magnetically non-equivalent phosphorus nuclei. Furthermore, the spin−spin coupling constant (J_{PP}) remains invariant for any arylboronic acid (J_{PP} = 37 Hz in $CDCl_3$). This last point suggests that the local P−Pd−P environment of the new compound should not be strongly modified with respect to complex **1**. These data are in agreement with the structural features computed for **1** and **2** reported in Table 1 and previously discussed.

In order to further confirm the consistency of the experimental data with the theoretically postulated structure of **2**, NMR calculations were also performed for complexes **1** and **2**.

If one simply computes the spectra by using the optimized geometry of **1,** the calculated spectrum yields two phosphorus nuclei magnetically non-equivalent, whereas these nuclei are magnetically equivalent in experiments. This result is due to the fact the NMR calculation is realized on a frozen structure, the optimized one, of the peroxo complex **1** where the internal rotation of the phosphines around the Pd−P, allowed at room temperature, is not taken into account. As a consequence, the chemical environment of the two phosphorus nuclei is artificially

TABLE 1: Selected Structural Parameters Computed for 1 and 2 (as a Function of Z) with Respect to the Available Experimental Data for 1[a,b]

	1					
	d(O−O)	d(Pd−O)	d(Pd−O)	θ(PPdP)	d(O_a−B)	d(Pd−P)
computed	1.429	2.043	2.061	105.9		2.396/2.400
exp[a]	1.421	1.999	2.013	102.5		2.272/2.295
	2					
	d(O_a−O_b)	d(Pd−O_a)	d(Pd−O_b)	θ(PPdP)	d(O_a−B)	d(Pd−P_a)/d(Pd−P_b)
Z = MeO	1.452	2.128	2.024	104.5	1.653	2.374/2.363
Z = H	1.452	2.123	2.025	104.2	1.650	2.375/2.364
Z = CN	1.455	2.136	2.021	104.4	1.642	2.374/2.362

[a] X-ray structure from Cambridge Crystallographic Data Centre (CCDC Deposit number 235181). [b] Distances d in angstoms and angles θ in degrees; refer to Figure 3 for labelling.

TABLE 2: Formation Energies (ΔE) and Enthalpies (ΔH) Computed for 2 as a Function of the Substituent (Z) on the Arylboronic Acid (All Values in kJ/mol)

Z	ΔE	ΔH
MeO	−28.1	−26.8
H	−33.1	−31.8
CN	−51.3	−49.4

TABLE 3: Computed (^{11}B and ^{31}P) and Experimental (^{31}P) NMR Chemical Shifts (δ in ppm) of 2

A	computed ($^{31}P_a$/$^{31}P_b$)	experimental[a]	computed[b] ^{11}B
Z=MeO	25.3/23.3	31.1 / 27.3	−4.2
Z=H	28.8/24.9	31.2 /27.3	−4.3
Z=CN	28.3/23.3	31.6 / 27.6	−5.2
1[c]	33.2	33.2	-

[a] In $CDCl_3$ from ref 10. [b] Chemical shift with respect to corresponding isolated boronic acid. [c] Theoretical value scaled to experimental reference, see text for details.

TABLE 4: Vibrational Stretching Frequency (ν_{O-O}, in cm^{-1}) Computed for 1 and 2[a]

compound	ν_{O-O}
1	999 (875)
2 (Z = OMe)	947
2 (Z = H)	947
2 (Z = CN)	942

[a] Available experimental data in parenthesis.[30]

SCHEME 3

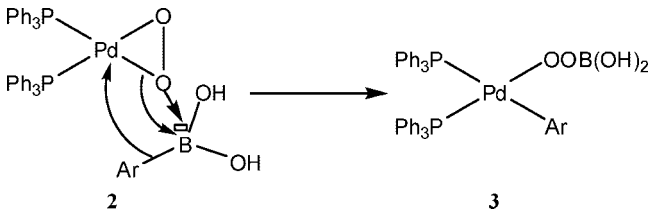

2 **3**

not the same; therefore, their chemical shifts become non-equivalent. In order to avoid such an artifact, the value of the isotropic shielding constant for each phosphorus nuclei has been calculated as a Boltzmann average (at T = 298 K) of the different conformers (eclipsed and staggered) that the peroxo complex **1** can assume as a function of the relative orientation of the two phosphines. The structures of the two conformers were obtained by a rigid rotation around the Pd−P bond, thus keeping all other structural parameters fixed to the corresponding optimized values.

In such a way, an average, equivalent value of the isotropic shielding constant is obtained for each of the phosphorus nuclei, confirmed to be magnetically equivalent. In table 3, the value of the chemical shift computed for **1** has been set equal to the experimental one, measured in $CDCl_3$, to allow for comparison between theoretical and experimental chemical shifts computed for **2**.

Contrary to complex **1**, in the case of system **2**, no averaging procedure has been applied to compute ^{31}P shielding constants, the values being obtained directly from the optimized structure. In this case, on the one hand, the rotation of the phosphine ligand around the Pd−P_a bond (refer to Figure 3) is completely hindered by the steric interaction between the hydrogen atoms of the hydroxyl groups of the boronic acid and the carbon atoms of the phenyl groups of the PPh_3; thus, no averaging is made for the chemical shift of the P_a nucleus. On the other hand, it has been tested, in the case of phenyl-boronic acid, that $\sigma(P_b)$ is practically insensitive to the relative phosphines' conformation. For these reasons, the values reported in Table 3 for complex **2** were not averaged.

The other technical problem related to the calculation of the chemical shift of ^{31}P within complexes **1** and **2** is linked to the choice of the basis set. Although purposely tailored basis sets for NMR calculation exist,[27] their size is normally very large so that NMR calculations for large systems (such as **1** and **2**) become unaffordable with these bases.

Because our aim was mainly to follow the shift to lower resonance frequencies of ^{31}P when going from the peroxo complex **1** to complex **2** and not their absolute value, we decided to use a relatively small basis set composed by a 6-311+G(d) basis for phosphorus atoms and all other heteroatoms (i.e., O and B),[28] the MIDI! basis[29] for all carbon and hydrogen atoms, and keeping the LANL2 basis and corresponding pseudopotential for the Pd atom. A validation of this mixed basis set was performed by computing the convergence of the ^{31}P chemical shift for an isolated PPh_3 molecule. The details of the validation are given as Supporting Information (Table SI.1).

An overall good agreement between computed and experimental data can be found by analyzing the results reported in Table 3. In particular, upon formation of complex **2**, independently from the Z substituent of the arylboronic acid, the phosphorous nuclei resonance frequencies are both shifted to lower values. Indeed, from the computed values, it is possible to attribute the lowest resonance frequency the phosphorous nuclei (P_b) in trans position to the oxygen directly coordinated to the boron atom (i.e., O_a, refer to Figure 3). Therefore, the difference in chemical shift between P_b and P_a upon formation

SCHEME 4

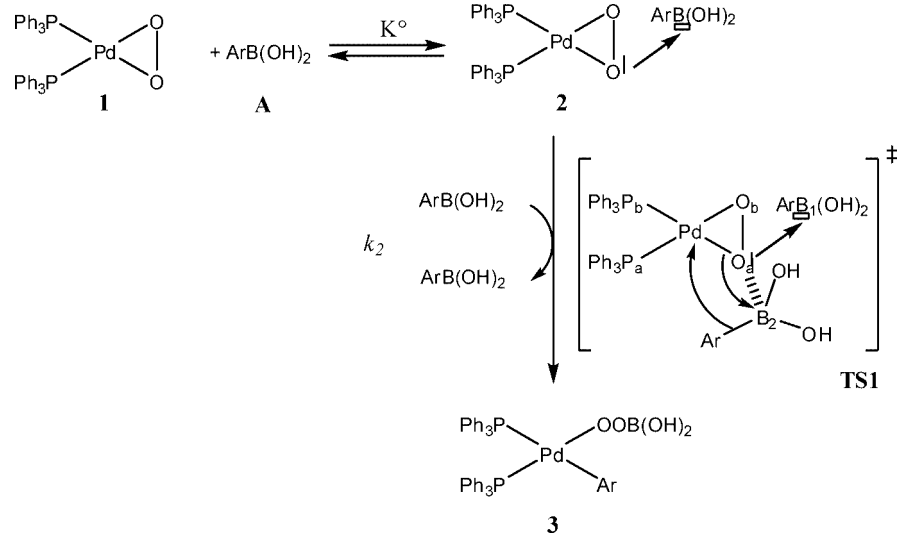

of **2** can be attributed to a standard trans effect. This effect is enhanced by the Lewis acidity of the boron atom, so that the largest computed and experimental $\Delta(\delta(P_b)-\delta(P_a))$ is obtained in the case of the 4-cyanophenylboronic acid. Nevertheless, the calculation overestimated the effect of the enhancement in acidity due to the presence of a cyano substituent most probably because of the neglecting of solvent effect.

Finally, one could expect that it is possible to further confirm the formation of **2** from the analysis of ^{11}B NMR spectra. Indeed, we expect that because of the formation of the oxygen−boron bond, the resonance frequency of the boron nuclei in complex **2** should be shifted to lower values with respect to the corresponding isolated boronic acid. This expectation is reflected by the computed data (Table 3), and in line with the Lewis acidity of the systems, the highest shift (−5.2 ppm) is computed for the cyano substituent. Unfortunately, experimentally, it has been shown that at room temperature, the formation of complex **2** leads only to the disappearance of the broad singlet due to the arylboronic acid without appearance of other signals.[10,30] This phenomena is consistent with equilibrium between **1** and **2,** the average signal obtained being too large to be observed at room temperature, and it does not allow us to further confirm the formation of **2**.

Finally, from a spectroscopic point of view, the formation of **2** could be validated by monitoring the variation in the O−O vibrational stretching frequency (ν_{O-O}) when going from the peroxo complex **1** to **2**. Indeed, it has been experimentally found that peroxo complexes where one of the oxygen atoms interacts with an electrophile display a significant shift (to lower frequencies) of ν_{O-O}.[31] The computed ν_{O-O} frequencies, reported in Table 4, correctly reproduce this expectation because in all cases, the formation of **2** leads to a shift of ν_{O-O} to lower frequencies of almost 50 cm^{-1}, the largest deviation with respect to the free peroxo complex **1** being computed for the most electrophilic substituent (CN).

Unfortunately, it was not possible to get further confirmation from experiments because it was experimentally impossible to follow the formation of **2** by IR measurements.[30]

Step 2: Aryl Transfer (from 2 to 3). Once the dative complex **2** is formed, the next step corresponds to the transfer of the aryl group from arylboronic acid to the palladium center. One could propose that the organoborate species **2** could undergo an intramolecular transmetallation reaction to yield complex **3,** as depicted in Scheme 3.

For this mechanism, the reaction rate should be independent of the concentration of **A** in solution. However, we have experimentally demonstrated[10,30] that the consumption rate of the starting peroxo complex **1** is proportional to $[\mathbf{1}]^1[\mathbf{A}]^2$. Because trimolecular reactions are quite uncommon in chemistry, it was interesting to understand why two equivalents of arylboronic acids are needed. To rationalize the reaction order in arylboronic acid, we thus have proposed a two-step mechanism starting from the peroxo complex **1** (Scheme 4).[10]

From the structural insights that we got on complex **2**, we can assume that its formation is the key step for the activation of the peroxo complex **1**. Indeed, the computed lengthening of the Pd−O bond (0.10 Å) dramatically increases the reactivity of both the palladium center and the oxygen atoms. Therefore, once the complex is activated (formation of **2**), we can suppose that a second equivalent of arylboronic acid can react on the palladium center with a reaction mechanism similar to a transmetallation reaction (Scheme 4): the aryl group of the second equivalent of arylboronic acid is transferred to the palladium coordination sphere in a concerted step. This reaction proceeds through a four-center transition state that involves the Pd, the activated oxygen atom (O_a), the boron atom of the second arylboronic acid (B_2), and the ipso carbon of the aryl substituent. During the step, an equivalent of boronic acid is released.

Because the coordination of a second molecule of arylboronic acid into the coordination sphere of the palladium introduces some steric crowding, in order to reduce this repulsive steric

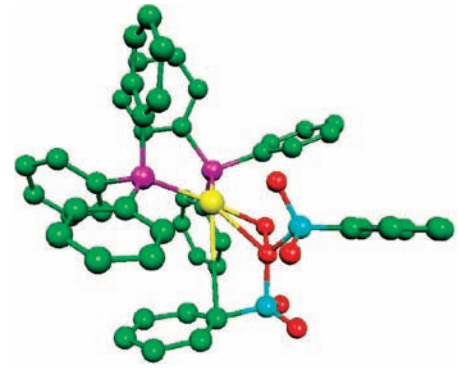

Figure 4. Schematic representation of the optimized structure of **TS1**. Hydrogen atoms are omitted for clarity.

TABLE 5: Main Structural Parameters Computed for TS1 and 3 (Distances in Angtroms)

TS1				
$d(Pd-P_a)/d(Pd-P_b)$	$d(Pd-O_a)/d(Pd-O_b)$	$d(O_a-O_b)$	$d(Pd-Ar)$	$d(B_2-O_a)/d(B_1-O_b)$
2.386/2.376	2.434/1.964	1.458	3.598	1.695/1.713
3				
d(Pd−P)[a]/d(Pd−P)[b]	d(Pd−O)	d(O−O)	d(Pd−Ar)	d(B−O)
2.393/2.558	2.050	1.502	2.019	1.395

[a] Cis with respect to $-OOB(OH)_2$. [b] Trans with respect to $-OOB(OH)_2$.

interaction, it was chosen to approach the arylboronic acid to the palladium center from the less hindered face. By approaching the second equivalent of acid in such a way, we were able to locate a transition state corresponding to the postulated four-center transition state, the structure of which is reported in Figure 4. This species (**TS1**) is computed, in the gas phase, to be only 27.5 kJ/mol higher in energy than complex **2**, so that the reaction is feasible at room temperature.

From the analysis of the main structural parameters of **TS1**, collected in Table 5, it can be noted that the Pd−P distances are only slightly affected by the coordination of the second equivalent of boronic acid, the variation with respect to complex **2** being of the order of 0.01 Å. On the contrary, the Pd−O bond lengths are significantly modified: the activated oxygen (O_a, refer to Scheme 4 for labelling) almost leaves the coordination sphere of Pd ($d(Pd-O_a) = 2.434$ Å), in agreement with the postulated reaction mechanism. As expected, the oxygen−oxygen bond is not modified ($d(O_a-O_b) = 1.458$ Å, $\nu_{O-O} = 947$ cm^{-1} with respect to $d(O_a-O_b) = 1.452$ Å, $\nu_{O-O} = 947$ cm^{-1} for **2**), in agreement with the postulated peroxo nature of dioxygen also in the transition state.

The boron oxygen distances slightly increase with respect to **2**, the O_a-B_2 distance being the shortest (1.695 Å with respect to 1.713 Å computed for O_a-B_1). This finding is in agreement with the incipient formation of the O_a-B_2 bond and the release of the first arylboronic acid molecule ($ArB_1(OH)_2$). Still, the palladium−carbon distance is quite long (3.598 Å) compared to the value computed for the product **3** ($d(Pd-Ar) = 2.019$ Å). Nevertheless, the phenyl group is very slightly distorted out of plane, thus pointing out the presence of a C_{ipso} of sp3 consequence of the incipient formation of the Pd−C bond.

In summary, all the structural evidence, as well as the analysis of the normal mode corresponding to the imaginary frequency, are consistent with the formation of the postulated four-center transition state (**TS1**) involving two equivalents of arylboronic acid.

Finally, in the gas phase, the overall process, that is, the conversion of **1** to **3**, is computed to be strongly exothermic ($\Delta H = -80.0$ kJ/mol).

Step 3: From Complex 3 to Complex 5. The third step is the formation of the experimentally characterized complex **5**. This system could be used as a starting material for transmetallation reactions.[32] Complex **5** may be formed from **3** in a sequence of two reactions: a hydrolysis[33] of the peroxide ($-OOB(OH)_2$) and a cis−trans isomerization. In fact, the starting system (**3**) is a cis-configurated complex, whereas the final product (**5**) is trans one (Figure 5).

From a structural point of view, one can note that for cis complexes (**3** and **4b**), the phosphine ligand, which is trans with respect to $-OOB(OH)_2$ (or $-OH$), shows a larger Pd−P bond length (0.15 Å) than that of the trans to the aryl group (see Table 6). Analogously, the Pd−O bond increases (by 0.4 and 0.7 Å for $-OOB(OH)_2$ and $-OH$, respectively) when going from a trans conformation with respect to PPh_3 (complex **3** and **4b**) to a trans conformation with respect to the phenyl group (**4a** and **5**).

For both reactions, we did not attempt to follow the reaction path that is to localize the transition states, because we cannot rule out an important role played by the solvent. As a matter of fact, both isomerization and hydrolysis either involve directly the solvent or could imply a dissociative mechanism (i.e., the leaving of the Pd coordination sphere by one ligand). Thus, large errors are expected when using a modeling performed in the gas phase. Nevertheless, one can reasonably characterize the expected stable intermediates, when either the isomerization (**4a**) or the hydrolysis (**4b**) first takes place. The overall results obtained in the gas phase are summarized in Figure 5.

By supposing that the isomerization first takes place, it appears, as expected, that the trans isomer (**4a**) is more stable than the cis system **3** of roughly 35 kJ/mol. Nevertheless, the starting peroxide adduct (**3**) is computed to be more stable than the final product, the hydroxo complex **5**, by 15 kJ/mol in the gas phase. This last point is contrary to the experimental evidence because the only species characterized was **5**, whereas all attempts to isolate **3** were unsuccessful.[10] The same considerations hold if the hydrolysis takes place first, giving rise to an unstable cis hydroxo species (**4b**, 36 kJ/mol higher in energy than **3**), which subsequently isomerizes to yield **5**.

The discrepancy between computed and experimental results can be largely ascribed to the neglecting of solvent effect. As a matter of fact, relative energies of the stable species **3**, **4**, and **5**, as well as reactants such as water or $HOOB(OH)_2$, can be strongly influenced by the presence of a polar, and eventually protic, solvent. To get a flavor of this effect at reasonable computation cost, single-point calculations were performed on optimized gas-phase structures including the solvent as a continuum dielectric (CPCM model).[25] In such a way, the structural reorganization induced by the solvent is neglected, as well as direct solute−solvent interactions, and only the bulk effect of the solvent on the total energy is considered. Although crude, this simple modelling allows us to recover the experimental findings, as depicted in Figure 6. In particular, as expected, complex **5** is found to be more stable that **3** in water (−3.4 kJ/mol) and practically isoenergetic in less polar solvent, such as $CHCl_3$ (+0.2kJ/mol). On one hand, in the case of both cis complex (**3**) and trans complex (**4a**), the hydrolysis is computed to be an endothermic process, although the difference in energy is reduced by the presence of the solvent. On the other hand, the relative stability of cis and trans conformers is less affected by the introduction of the solvent, especially in the case of the OH substituent (**4b** with respect to **5**).

In summary, inclusion of solvent seems mandatory to correctly describe this reaction step and, in particular, the hydrolysis reaction. Indeed, the simplest approach here applied

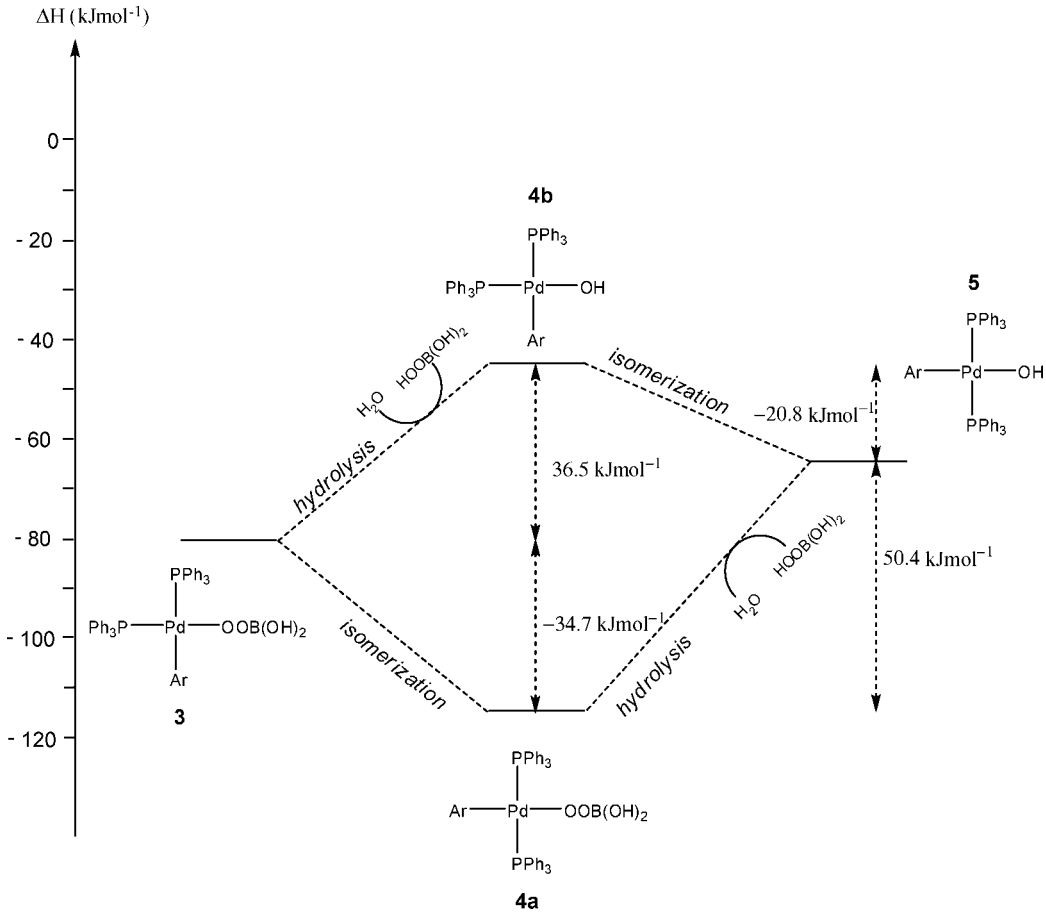

Figure 5. Relative stability of complex **3**, **4**, and **5** computed in the gas phase (relative energies in kJ/mol).

TABLE 6: Selected Structural Parameters Computed for Complexes 3, 4a, 4b, and 5 (Distances in Angtroms)

	3	4a	4b	5
d(Pd−O)	2.050	2.091	2.016	2.090
d(Pd−P)	2.393/2.558[a]	2.395/2.417	2.380/2.530[b]	2.396/2.381
d(Pd−Ar)	2.019	2.009	2.010	2.013

[a] Trans with respect to $-OOB(OH)_2$. [b] Trans with respect to −OH.

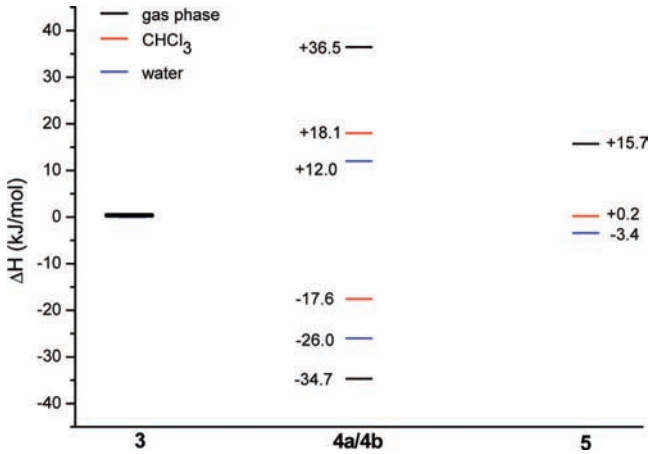

Figure 6. Relative stability of complex **4** and **5** with respect to complex **3** estimated in solution (blue, water and red, CH_3Cl) and in the gas phase (black). All energies are expressed in kJ/mol.

does not allow us to determine the transition states, by explicitly involving the solvent molecules or a dissociative mechanism, and thus can-not be used to define, if any, the preferred sequence for the hydrolysis and isomerization reactions.

Conclusion

DFT has been successfully applied to the analysis of the key elementary steps of an intermingled catalytic cycle such as the homocoupling of arylboronic acids catalyzed by palladium complexes. Theoretical insights have further validated the mechanism postulated on the basis of kinetic and spectroscopic experimental evidence, confirming the crucial role played by a joint theoretical and experimental approach.

In particular, the key role played by a Lewis acid−base adduct to activate the starting Pd-peroxo catalyst has been pointed out, as well as the importance of a four-center transition state to justify the uncommon kinetic law experimentally found for the starting reactions.[10]

Nevertheless, the present work also shows the limit of the selected computational approach, claiming for an explicit evaluation of solvent effects in order to better characterize the isomerization and hydrolysis steps. Further work, including dynamic and solvent effects seems, thus, compulsory to fully characterize the last part of the catalytic cycle.

Acknowledgment. This work has been supported in part by the Centre National de la Recherche Scientifique (UMR CNRS-ENS-UPMC 8640, UMR CNRS-ENSCP-UMPC 7575) and the Ministère de la Recherche (Ecole Normale Supérieure).

Supporting Information Available: Schematic structure of optimized systems, basis set dependence computed for the ^{31}P

shielding constant of PPh_3, and complete ref 14. This material is available free of charge via the Internet at http://pubs.acs.org.

References and Notes

(1) For a recent review on the synthesis of biaryls, see Hassan, J.; Sevignon, M.; Gozzi, C.; Schulz, E.; Lemaire, M. *Chem. Rev.* **2002**, *102*, 1359–1469.

(2) (a) Miyaura, N.; Yanagi, T.; Suzuki, A. *Synth. Commun.* **1981**, *11*, 513–519. For reviews, see (b) Suzuki, A. *Pure Appl. Chem.* **1991**, *63*, 419–422. (c) Miyaura, N.; Suzuki, A. *Chem. Rev.* **1995**, *95*, 2457–2483. (d) Suzuki, A. *J. Organomet. Chem.* **1999**, *576*, 147–168. (e) Miyaura, N. Synthesis of biaryls via the cross-coupling reaction of arylboronic acids. *Advances in Metal-Organic Synthesis*. JAI Press Inc.: London, 1998; Vol. 6, pp 187−243.

(3) (a) Campi, E. M.; Jackson, R.; Marcuccio, S.; Naeslund, C. G. M. *J. Chem. Soc. Chem. Commun.* **1994**, 2395–2395. (b) Gillmann, T.; Weeber, T. *Synlett* **1994**, 649–651. (c) Song, Z. Z.; Wong, H. N. C. *J. Org. Chem.* **1994**, *59*, 33–41.

(4) (a) Wong, M. S.; Zhang, X. L. *Tetrahedron Lett.* **2001**, *42*, 4087–4089. (b) Kabalka, G. W.; Wang, L. *Tetrahedron Lett.* **2002**, *43*, 3067–3068. (c) Koza, D. J.; Carita, E. *Synthesis* **2002**, 2183–2186.

(5) (a) Moreno-Mañas, M.; Pérez, M.; Pleixats, R. *J. Org. Chem.* **1996**, *61*, 2346–2351. (b) Aramendia, M. A.; Lafont, M.; Moreno-Mañas, M.; Pérez, M.; Pleixats, R. *J. Org. Chem.* **1999**, *64*, 3592–3594.

(6) (a) Smith, C. A.; Campi, E. M.; Jackson, R.; Marcuccio, S.; Naeslund, C. G. M.; Deacon, G. B. *Synlett* **1997**, 131–132. (b) Parrish, J. P.; Jung, Y. C.; Floyd, R. J.; Jung, K. W. *Tetrahedron Lett.* **2002**, *43*, 7899–7902.

(7) Yoshida, H.; Yamaryo, Y.; Ohshita, J.; Kunai, A. *Tetrahedron Lett.* **2003**, *44*, 1541–1544.

(8) Sheldon, R. A.; Kochi, J. K. Activation of Molecular Oxygen by Metal Complexes. *Metal-catalyzed Oxidations of Organic Compounds*, Academic Press: New-York, 1981; Chapter 4, pp 71−119.

(9) For a review on palladium peroxo complexes as intermediates in catalytic reactions, see Stahl, S. S. *Angew. Chem. Int. Ed.* **2004**, *43*, 3400–3420.

(10) Adamo, C.; Amatore, C.; Ciofini, I.; Jutand, A.; Lakmini, H. *J. Am. Chem. Soc.* **2006**, *128*, 6829.

(11) (a) Koch, W.; Holthausen, M. C. *A Chemist's Guide to Density Functional Theory of Atoms and Molecules*; Wiley-VCH: Weinheim, 2000. (b) Parr, R. G.; Yang, W. *Density Functional Theory of Atoms and Molecules*; Oxford University Press: New York, 1989.

(12) (a) For recent references, see for instance. Drees, M.; Strassner, T. *Inorg. Chem.* **2007**, *46*, 10850–10859. (b) Celik, M. A.; Yurtsever, M.; Tuzun, N. S.; Gungor, F. S.; Sezer, O.; Anac, O. *Organometallics* **2007**, *26*, 2978–2985. (c) Privalov, T.; Samec, J. S. M.; Backvall, J.-E. *Organometallics* **2007**, *26*, 2840–2848. (d) Fan, Y.; Gao, Y. Q. *J. Am. Chem. Soc.* **2007**, *129*, 905–913. (e) Hirao, H.; Que, L.; Nam, W.; Shaik, S. *Chem. Eur. J.* **2008**, *14*, 1740–1756. (f) Cohen, S.; Kozuch, S.; Hazan, C.; Shaik, S. *J. Am. Chem. Soc.* **2006**, *128*, 11028–11029. (g) Rondinelli, F.; Russo, N.; Toscano, M. *Inorg. Chem.* **2007**, *46*, 7489–7493. (h) Leopoldini, M.; Russo, N.; Toscano, M. *J. Am. Chem. Soc.* **2007**, *129*, 7776–7784.

(13) (a) Kozuch, S.; Shaik, S.; Jutand, A.; Amatore, C. *Chem. Eur. J.* **2004**, *10*, 3072–3080. (b) Amatore, C.; Jutand, A.; Lemaître, F.; Ricard, J.-L.; Kozuch, S.; Shaik, S. *J. Organomet. Chem.* **2004**, *689*, 3728–3734. (c) Kozuch, S.; Amatore, C.; Jutand, A.; Shaik, S. *Organometallics* **2005**, *24*, 2319–2330.

(14) Frisch, M. J.; Trucks, G. W.; Schlegel, H. B.; Scuseria, G. E.; Robb, M. A.; Cheeseman, J. R.; Montgomery, J. A., Jr.; Vreven, T.; Kudin, K. N.; Burant, J. C.; Millam, J. M.; Iyengar, S. S.; Tomasi, J.; Barone, V.; Mennucci, B.; Cossi, M.; Scalmani, G.; Rega, N.; Petersson, G. A.; Nakatsuji, H.; Hada, M.; Ehara, M.; Toyota, K.; Fukuda, R.; Hasegawa, J.; Ishida, M.; Nakajima, T.; Honda, Y.; Kitao, O.; Nakai, H.; Klene, M.; Li, X.; Knox, J. E.; Hratchian, H. P.; Cross, J. B.; Bakken, V.; Adamo, C.; Jaramillo, J.; Gomperts, R.; Stratmann, R. E.; Yazyev, O.; Austin, A. J.; Cammi, R.; Pomelli, C.; Ochterski, J. W.; Ayala, P. Y.; Morokuma, K.; Voth, G. A.; Salvador, P.; Dannenberg, J. J.; Zakrzewski, V. G.; Dapprich, S.; Daniels, A. D.; Strain, M. C.; Farkas, O.; Malick, D. K.; Rabuck, A. D.; Raghavachari, K.; Foresman, J. B.; Ortiz, J. V.; Cui, Q.; Baboul, A. G.; Clifford, S.; Cioslowski, J.; Stefanov, B. B.; Liu, G.; Liashenko, A.; Piskorz, P.; Komaromi, I.; Martin, R. L.; Fox, D. J.; Keith, T.; Al-Laham, M. A.; Peng, C. Y.; Nanayakkara, A.; Challacombe, M.; Gill, P. M. W.; Johnson, B.; Chen, W.; Wong, M. W.; Gonzalez, C.; Pople, J. A. *Gaussian 03*; Gaussian, Inc.: Wallingford, CT, 2003.

(15) Adamo, C.; Barone, V. *J. Chem. Phys.* **1999**, *110*, 6158–6170.

(16) Perdew, J. P.; Burke, K.; Ernzerhof, M. *Phys. Rev. Lett.* **1996**, *77*, 3865–3868.

(17) Adamo, C.; Barone, V. *Chem. Phys. Lett.* **1997**, *274*, 242–250.

(18) Dunning, T. H., Jr.; Hay, P. J. In *Modern Theoretical Chemistry*; Schaefer, H. F., III., Ed.; Plenum: New York, 1976, pp 1−28.

(19) Hay, J.; Wadt, W. R. J. *Chem. Phys.* **1985**, *82*, 299–310.

(20) See for instance (a) Ciofini, I.; Lainé, P. P.; Bedioui, F.; Adamo, C. *J. Am. Chem. Soc.* **2004**, *126*, 10763–10777. (b) Mawhinney, R. C.; Peslherbe, G. H.; Muchall, H. M. *J. Phys. Chem. B* **2008**, *112*, 650–655. (c) Fomine, S.; Tlenkopatchev, M. A. *Organometallics* **2007**, *26*, 4491–4497. (d) Zenkina, O.; Altman, M.; Leitus, G.; Shimon, L. J. W.; Cohen, R.; van der Boom, M. E. *Organometallics* **2007**, *26*, 4528–4534.

(21) Basis-set superposition errors were evaluated by using the standard Counterpoise correction, the largest being of the order of 6 kcal/mol. To test basis-set dependence of energetic and structural features, additional calculations were performed by using a larger basis set only on O, P, and B atoms in order to test basis-set dependence for the formation of **2**. In particular, it was shown that the same qualitative results are obtained with a Pople triple-zeta basis including polarization function on these atoms (6-311G(d)). The same holds when adding a diffuse function on oxygen atoms (i.e. 6-311+G(d)). Therefore, if not differently specified, all values correspond to those obtained with the LANL2DZ basis.

(22) Ditchfield, R. *Mol. Phys.* **1974**, *27*, 789.

(23) Miertus, S.; Scrocco, E.; Tomasi, J. *Chem Phys.* **1981**, *55*, 117.

(24) Cossi, M.; Barone, V.; Cammi, R.; Tomasi, J. *Chem. Phys. Lett.* **1996**, *255*, 327.

(25) Barone, V.; Cossi, M. *J. Chem. Phys. A* **1998**, *102*, 1995.

(26) Liu, X.-C.; Hubbard, J. L.; Scouten, W. H. *J. Organomet. Chem.* **1995**, *493*, 91.

(27) See for instance Kutzelnigg, W.; Fleischer, U. ; Schindler, M. *NMR Basic Principles and Progress*; Springer-Verlag: Berlin, 1990; p 165.

(28) Krishnan, R.; Binkley, J. S.; Seeger, R.; Pople, J. A. *J. Chem. Phys.* **1980**, *72*, 650.

(29) Easton, R. E.; Giesen, D. J.; Welch, A.; Cramer, D. J.; Truhlar, D. G. *Theor. Chim. Acta* **1996**, *93*, 281.

(30) Lakmini, H. Etudes mécanistiques de réactions catalysées par des complexes de palladium mettant en jeu des réactifs organoborés: Homocouplage et coupage croisé. Ph.D. thesis, Université Pierre et Marie Curie, Paris 6, Paris, 2006.

(31) Mimoun, H.; Saussine, L.; Daire, E.; Postel, M.; Fischer, J.; Weiss, R. *J. Am. Chem. Soc.* **1983**, *105*, 3101.

(32) (a) For hypothetical reactions of $ArPd(OH)L_2$ with arylboronic acids, see ref 2c. (b) For reactions and kinetic data, see Amatore, C.; Boubekeur-Lecaque, L.; Jutand, A. 2008, unpublished results. (c) For DFT calculations, see Braga, A. A. C.; Morgon, N. H.; Ujaque, G.; Lledos, A.; Maseras, F. *J. Organomet. Chem.* **2006**, *691*, 4459–4466.

(33) Even if all experiments have been performed in anhydrous conditions, the presence of water cannot be excluded because of the equilibrium between arylboronic acid and its boroxine.

JP801948U